Plasmonics (2015) 10:949–954
DOI 10.1007/s11468-015-9884-7

Rolled-Up Ag-SiO_x Hyperbolic Metamaterials for Surface-Enhanced Raman Scattering

Yan Zhang · Di Han · Deyang Du · Gaoshan Huang · Teng Qiu · Yongfeng Mei

Received: 5 November 2014 / Accepted: 4 January 2015 / Published online: 1 March 2015

Abstract A convenient technique is reported to fabricate Ag-SiO_x hyperbolic metamaterials (HMMs) as robust surface-enhanced Raman scattering (SERS) substrates based on roll-up nanotechnology. As an illustration, dramatic enhancement is achieved using Rhodamine 6G as a molecular probe, which indicates that a larger plasmonic density of states exist, leading to a greatly enhanced local electromagnetic (EM) field when the sample is irradiated with a laser beam. Optimized results are obtained by controlling the thickness of alumina coating onto Ag-SiO_x HMMs using atomic layer deposition. Finite-difference time-domain simulations further illustrate the excitation of localized surface plasmon modes by calculating the EM field properties on the surface of Ag-SiO_x HMMs. This efficient method of producing Ag-SiO_x HMMs with highly SERS-active properties could spur expanding applications in metamaterials and bioanalysis.

Keywords Surface-enhanced Raman scattering · Hyperbolic metamaterials · Roll-up nanotechnology · Microtube

Yan Zhang and Di Han contributed equally.

Electronic supplementary material The online version of this article (doi:10.1007/s11468-015-9884-7) contains supplementary material, which is available to authorized users.

Y. Zhang · D. Han · D. Du · T. Qiu (✉)
Department of Physics, Southeast University, Nanjing 211189, People's Republic of China
e-mail: tqiu@seu.edu.cn

G. Huang · Y. Mei (✉)
Department of Materials Science, Fudan University, Shanghai 200433, People's Republic of China
e-mail: yfm@fudan.edu.cn

Introduction

Nanotechnology allows for the creation of material properties which cannot be found in nature [1–3], and these materials have been referred to as metamaterials [4, 5]. The macroscopic optical parameters (effective permittivity, permeability, refractive index, impedance) of such media can be made to enter highly unusual regimes, which leads to completely surprising results, such as the ability of a planar slab of a negative index metamaterial to focus lightwaves without an intrinsic limit to resolution, or the possibility to stop and localize light pulses in plasmonic heterostructures [5]. In particular, hyperbolic metamaterials (HMMs), composed of a stack of metal-dielectric multilayers, are especially promising because of their unique hyperbolic dispersion relation, which leads to a larger plasmonic density of states (DOS) [6–10]. Engineering plasmonic DOS using outcoupling nanostructures in multilayer HMMs can provide desired tunability of Purcell factor enhancement for light emission, with both high speed and high radiative intensity at broadband operational frequencies, for applications in biosensing, light-emitting devices, and surface-enhanced Raman scatting (SERS) [8–10]. For example, Sechrist et al. theoretically proved the electric field enhancement from a nanowell array etched into a metal-dielectric multilayer, which should produce very high Raman enhancement [11]. Prokes et al. systematically investigated the hyperbolic and plasmonic properties of silicon nanowire/Ag arrays; the measured SERS signals were enhanced due to plasmonic coupling of closely spaced nanowires and enhanced photonic DOS in HMMs [12]. However, the difficulties in fabricating metal-dielectric multilayers with 3D fine structures limit the practical application, especially in optofluidics.

Self-assembled rolled-up nanostructures, with good control of morphology and high specificity by using roll-up nanotechnology [13], have provided substantial advancements in electronics [14], magnetics [15], fluidics [16, 17], photonics

[18–20], and other relevant research fields [21]. Herein, we propose a way in which roll-up nanotechnology opens the door for fabricating metal-dielectric HMMs. Pre-stressed metal-dielectric nanomembranes deposited onto a polymer sacrificial layer are released from the substrate surface by removing the sacrificial layer with a solvent and roll-up into a microtube to form curved metal-dielectric multilayers structure, which can function as an optofluidic channel and even show more efficiency in exciting localized surface plasmon (LSP) modes than flat one according to previous research [20].

In this work, we design and fabricate Ag-SiO_x HMMs based on metal-dielectric composite microtubes by employing roll-up nanotechnology [22]. This multilayer combination is selected based on the optical properties, the compatibility of film growth and the feasibility of roll-up process. Pronounced SERS is observed, which indicates that a larger plasmonic DOS is existed, leading to an enhanced local electromagnetic (EM) field when the composite microtube surface is irradiated with a laser beam. In addition, a finite-difference time-domain (FDTD) method is employed to illustrate the excitation of LSP modes by calculating the EM field properties on the mircotube surface. Further improvements can be obtained by optimizing the thinkness of alumina layer, which is coated onto Ag-SiO_x HMMs using atomic layer depostion (ALD).

Experimental Details

Ag-SiO_x HMMs were fabricated by roll-up nanotechnology on a photoresist. The process was initiated by spin-coating a photoresist layer (ARP-3510 T positive resist) with a thickness of ~2 μm onto a Si substrate. Standard photolithography [23] was employed to pattern the photoresist layers into well-defined squares (80×80 μm^2). Subsequently, thin silver and SiO_x layers were deposited by electron beam evaporation with a tilt angle of 60° (Fig. 1a). By employing such a glancing angle deposition technique [24], a predefined rolling direction of the nanomembrane was introduced, because a shadow was created at one side of the photoresist edge that provides a well-defined starting line for the formation of rolled-up tubes (Fig. 1b). Ultimately, the photoresist layer was selectively removed by acetone. Simultaneously, intrinsic stress gradients across the deposited layers acted as a driving force to precisely release Ag-SiO_x nanomembranes into rolled-up microtubes, forming curved metal-dielectric multilayers structure (Fig. 1c). The microtubes were dried in the critical point dryer (Leica, CPD030) by using liquid CO_2 as intermedia to avoid collapse. It should be noted here SiO_x (SiO/SiO_2) bi-layer is selected as a basic rolling framework because of the two materials' readily available stress misfit for scrolling [22, 25].

Alumina films were deposited on freshly prepared Ag-SiO_x composite microtubes by ALD. The alumina precursor, trimethylaluminum (TMA) and high-purity water were

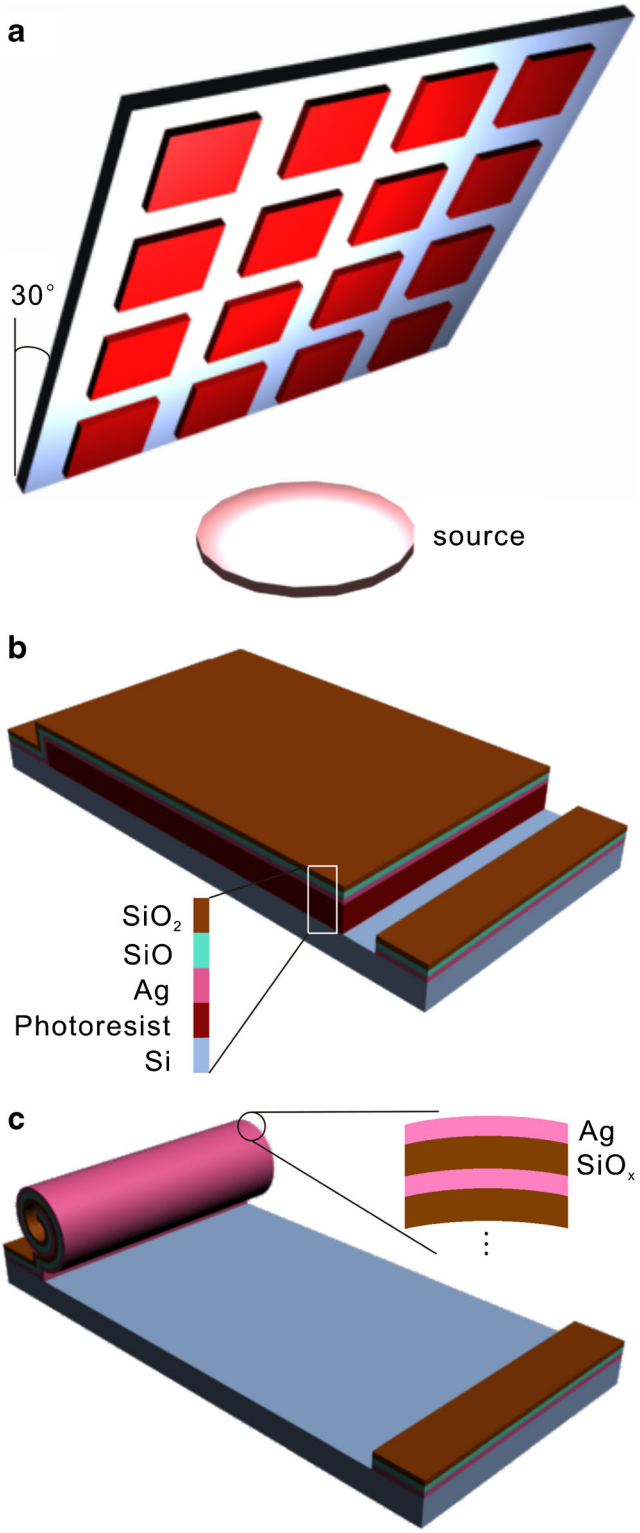

Fig. 1 Schematic of the fabrication process of Ag-SiO_x HMMs. **a** Photoresist layer pattern on Si substrate for glancing angle deposition. **b** Silver and SiO_x deposited on the photoresist layer with a narrow gap at the far end due to the ballistic shadow effect. **c** Selective removal of the photoresist layer with acetone and rolling up of the Ag-SiO_x nanomembrane to form metal-dielectric multilayers structure

alternately pumped to the reaction chamber using nitrogen as a carrier gas. Growth of alumina was achieved with an average growth rate of ~1.1 Å/cycle at 150 °C.

Scanning electron microscopy (SEM, JEOL JSM-6335F) was used to investigate the nanostructures. Raman measurements were performed with a Jobin Yvon LabRAM HR800 micro-Raman spectrometer using a 514-nm laser line at room temperature. An area ~1 μm in diameter was probed with a 50× objective lens, and the incident power at the sample was 0.005 mW. The signal collection time was 10 s. To evaluate the substrate Raman-enhancing capability, an aqueous solution of rhodamine 6G (R6G) was prepared and dispensed on the samples to facilitate molecular absorption. It should be noted that the acquisition time and laser power were the same for all Raman spectra.

Commercial FDTD software (CST MWS 2010) was used to calculate the EM field properties of nanostructures. The Drude model was employed to describe the properties of the materials. The parameters of the composite microtubes in the simulation were set to the parameters in our experiments. The wavelength of the incident wave was set to 514 nm.

Results and Discussion

A typical SEM image of a bare microtube array patterned into well-aligned squares with the same rolling direction is shown in Fig. 2a. The ability to align tubes in a highly ordered manner demonstrates that variously shaped tube patterns can be readily constructed by controlling the geometries and positions of the photoresist layers by standard photolithography processes. Moreover, employing polymer as the photoresist layer allows for simple removal of the underlying sacrificial layer without dissolution of the nanomembrane material itself during the underetching process [22]. A tunable film thickness can be achieved by varying the deposition time of electron beam evaporation, and due to the existence of intrinsic stress in the multilayer structure, the free-standing films bend up and self-assemble into a tubular structure. The driving force for tube formation can be controlled by changing the deposition parameters, such as growth rate and substrate temperature [22]. It is worth noting that the rotation number of microtubes varying with the film thickness, stress gradient, and etching time provides an advantage in tailoring the stacking number of metal-dielectric multilayers. The stacking number N can be calculated according to the simple equation $N=L/\pi D$, where L and D represent the length of nanomembrane and the diameter of microtube, respectively. Figure 2b shows an SEM image of a typical single microtube. The diameter of microtube is around ~5 μm, and calculation result of the stacking number is about 5. The prepared curved Ag-SiO_x HMMs have a smooth surface as can be illustrated by a typical atomic force microscopy (AFM) image (Fig. S1).

To evaluate the substrate Raman-enhancing capability, a 1×10^{-5} M aqueous solution of R6G was prepared and dispensed on the samples to facilitate molecular absorption. Figure 3a shows the typical Raman spectra of R6G molecules absorbed on the bare curved Ag-SiO_x HMM and a flat one. A silver film reference prepared by electron beam evaporation is also necessary, which represents a traditional SERS substrate. Many salient peaks were clearly observed when the R6G molecules were absorbed on the curved Ag-SiO_x HMM, and the pronounced peaks at 1362, 1507, 1574, and 1650 cm^{-1} can be assigned to the totally symmetric modes of in-plane C–C stretching vibrations [26]. The contrast of the quantitative enhancement (at 1650 cm^{-1}) is illustrated in the left projection drawing. Each data point represents the average intensity of repeated measurements, with the standard deviation shown by the error bars. Obviously, a comparison between the intensity of the Raman peaks of R6G on the curved HMM fabricated by roll-up nanotechnology and on the other references suggests that the curved metal-dielectric multilayers structure provides larger Raman enhancement, which, in turn, indicates that more LSP modes were excited on the surface.

It is commonly thought that EM enhancements make a major contribution to the SERS phenomenon [27]. When both

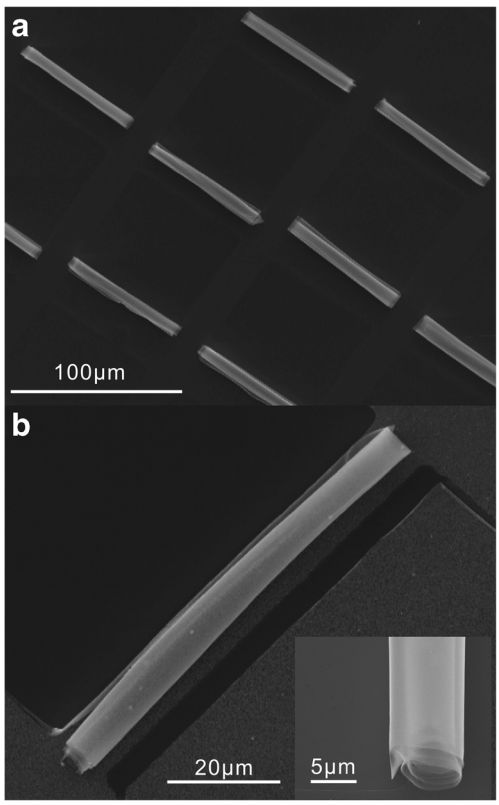

Fig. 2 **a** SEM image of a bare microtube array patterned into well-aligned squares with the same rolling direction. The layer thicknesses are set to 5, 5, and 20 nm for each silver, SiO, and SiO_2 layer, respectively. **b** SEM image of a typical single microtube with a diameter of ~5 μm

the incident light and the scattered signal of molecules are in resonance with the plasmon frequency, then the SERS signal is maximized, leading to the $|E|^4$ enhancement [28]. To assess the validity of our measurements, an FDTD method was used to calculate the local EM field, as shown in Fig. 3b–d. When irradiated by a laser beam, the LSP modes on the surface of cuverd Ag-SiO_x HMM lead to a larger EM field than the other references, in turn causing a significant Raman enhancement. The enhanced EM field near the top area was apparently larger under the laser beam vertically irradiating the top surface, whereas on the side faces, the interaction between incident light and free electrons on the metal surface was not as efficient as that on the top [20]. Normalized average SERS signal at 1650 cm^{-1} and the biquadrate of simulated maximum EM field intensity as a function of different structures were measured to verify the correlation between experiment and simulation, as shown in Fig. 3e.

According to the literatures [29, 30], the localized surface plasmon resonance of nanostructures is shown to exhibit a singularity when the surrounding dielectric medium exhibits amplification with a critical value of gain [29]. This composite

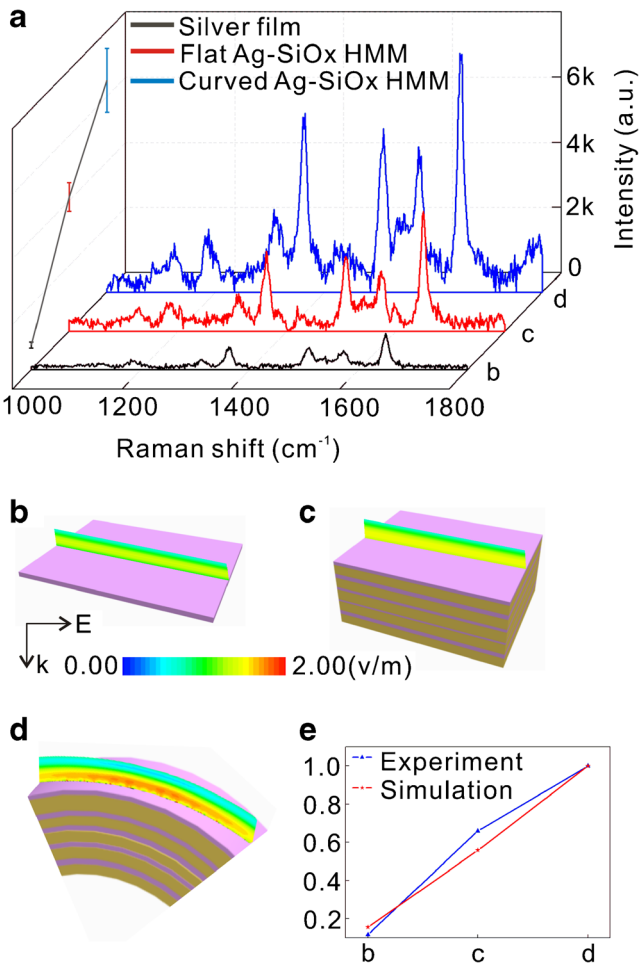

Fig. 3 **a** SERS spectral comparison of 10^{-5} M R6G adsorbed on the surface of the curved Ag-SiO_x HMM, flat Ag-SiO_x HMM, and a silver film. The left projection drawing shows the quantitative enhancement comparison at 1650 cm^{-1}. **b**–**d** Simulated EM field distribution maps of different structures. The 2-fold enhancement in the EM field does not represent the maximum electric field strength but is artificially set to provide better intuitive models of the EM field. **b** Silver film. **c** Flat Ag-SiO_x HMM. **d** Curved Ag-SiO_x HMM. **e** Normalized average SERS signal at 1650 cm^{-1} and the biquadrate of simulated maximum EM field intensity as a function of different structures: **b** silver film, **c** flat Ag-SiO_x HMM, and **d** curved Ag-SiO_x HMM

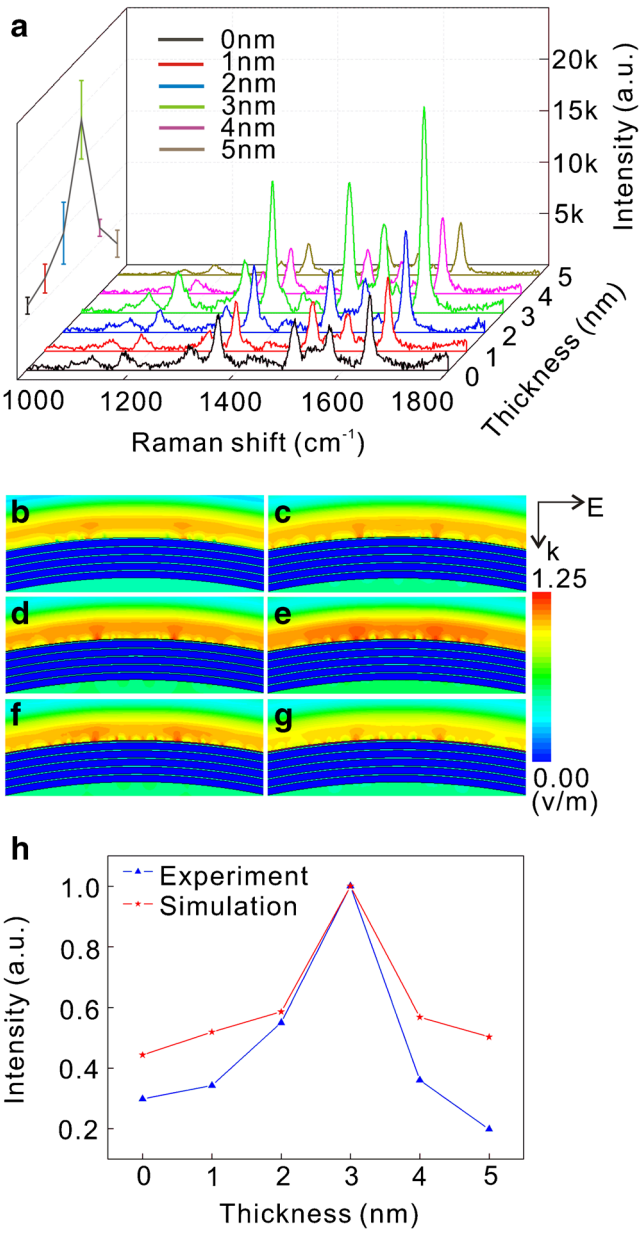

Fig. 4 **a** SERS spectra comparison of 10^{-5} M R6G adsorbed on the Ag-SiO_x HMMs coated with different thicknesses of alumina (0, 1, 2, 3, 4, 5 nm). The left projection drawing shows the quantitative enhancement comparison at 1650 cm^{-1}. **b**–**g** Simulated EM field distribution maps of Ag-SiO_x HMMs coated with different thicknesses of alumina (**b**: 0, **c**: 1, **d**: 2, **e**: 3, **f**: 4, **g**: 5 nm). The 1.25-fold enhancement in the EM field does not represent the maximum electric field strength but is artificially set to provide better intuitive models of the EM field. **h** Normalized average SERS signal at 1650 cm^{-1} and the biquadrate of simulated maximum EM field intensity as a function of alumina thickness

medium should exhibit strong scattering within the plasmon band leading to low threshold random laser action and light localization effects, which could also greatly increase surface-enhanced Raman scattering [29]. Hence, different thickness layers of alumina (1, 2, 3, 4 and 5 nm) were coated onto Ag-SiO_x HMMs by ALD to tune the SERS intensity. Raman measurements were acquired for a 6-μl aliquot of R6G (10^{-5} M) drop coated onto the five alumina-coated Ag-SiO_x HMMs and a bare Ag-SiO_x HMM. Figure 4a shows SERS spectra of R6G adsorbed on the six Ag-SiO_x HMMs coated with different thickness of alumina. Ten replicate SERS measurements were obtained from different areas of each substrate to ensure that the measured spectra accurately represented the true enhanced spectrum. The contrast of the quantitative enhancement (at 1650 cm^{-1}) is illustrated in the left projection drawing. Each data point represents the average intensity at 1650 cm^{-1}, with the standard deviation shown by the error bars. Interestingly, the SERS enhancement factor of R6G achieves a maximum of 4×10^5 when the Ag-SiO_x HMMs are modified with 3-nm thickness of alumina, then decreases with further addition of alumina [31]. Given that the SERS distance dependence studies [32], the EM field decays rapidly when the distance between the scatterers and the silver nanostructures increases, thus the result is a subtle combination between the theory of optical gain in dielectric and the distance dependence.

Furthermore, EM field distribution simulations of Ag-SiO_x HMMs coated with different thicknesses of alumina (0, 1, 2, 3, 4, 5 nm) were implemented, as shown in Fig. 4b–g. As the thickness of the coated alumina was increased from 0 to 3 nm, the theory of optical gain dominated and the EM field became stronger. While the thickness of coated alumina increased more, distance dependence ruled, resulting in a low enhancement. The biquadrate of simulated maximum EM field intensity as a function of alumina thicknesses is shown in Fig. 4h, which demonstrates good correlation with the experimental data. These results open a practical route toward achieving SERS-tunable Ag-SiO_x HMMs by simply changing the thickness of coated alumina using ALD.

Conclusion

In summary, we have reported a simple technique to fabricate Ag-SiO_x HMMs based on metal-dielectric composite microtubes by employing roll-up nanotechnology. Pronounced SERS was observed, indicating that LSP modes can be excited that lead to a greatly enhanced local EM field. Optimized results are obtained by controlling the thickness of alumina coating onto Ag-SiO_x HMMs using ALD. FDTD simulations further illustrate the excitation of LSP modes by calculating the EM field properties on the surface of Ag-SiO_x HMMs. This efficient method of producing Ag-SiO_x HMMs with highly SERS-active properties allows for expanding applications in metamaterials and bioanalysis.

Acknowledgments T.Q. acknowledges support from the National Natural Science Foundation of China under Grant No. 51271057, the Natural Science Foundation of Jiangsu Province, China, under Grant no. BK2012757 and the Program for New Century Excellent Talents in University of Ministry of Education of China under Grant no. NCET-11-0096. Y.F.M. and G.S.H. thank the support from the Natural Science Foundation of China (nos. 51322201 and 51475093) and Science and Technology Commission of Shanghai Municipality (nos. 12520706300 and 14JC1400200).

References

1. Pendry JB (2004) A chiral route to negative refraction. Science 306(5700):1353–1355
2. Liu ZW, Lee H, Xiong Y, Sun C, Zhang X (2007) Far-field optical hyperlens magnifying sub-diffraction-limited objects. Science 315(5819):1686
3. Smith EJ, Liu ZW, Mei YF, Schmidt OG (2010) Combined surface plasmon and classical waveguiding through metamaterial fiber design. Nano Lett 10(1):1–5
4. Soukoulis CM, Wegener M (2011) Past achievements and future challenges in the development of three-dimensional photonic metamaterials. Nat Photon 5:523–530
5. Hess O, Pendry JB, Maier SA, Oulton RF, Hamm JM, Tsakmakidis KL (2012) Active nanoplasmonic metamaterials. Nat Mater 11:573–584
6. Tumkur T, Zhu G, Black P, Barnakov YA, Bonner CE, Noginov MA (2011) Control of spontaneous emission in a volume of functionalized hyperbolic metamaterial. Appl Phys Lett 99:151115
7. Krishnamoorthy HNS, Jacob Z, Narimanov E, Kretzschmar I, Menon VM (2012) Topological transitions in metamaterials. Science 336(6078):205–209
8. Kim J, Drachev VP, Jacob Z, Naik GV, Boltasseva A, Narimanov EE, Shalaev VM (2012) Improving the radiative decay rate for dye molecules with hyperbolic metamaterials. Opt Express 20:8100–8116
9. Poddubny A, Iorsh I, Belov P, Kivshar Y (2013) Hyperbolic metamaterials. Nat Photon 7:958–967
10. Lu D, Kan JJ, Fullerton EE, Liu ZW (2014) Enhancing spontaneous emission rates of molecules using nanopatterned multilayer hyperbolic metamaterials. Nat Nanotech 9:48–53
11. Sechrist ZA, Tonucci RJ, Cambrea LR (2013) Stabilization of center frequency nanowell metamaterials for SERS applications. Appl Phys B 112:133–142
12. Prokes SM, Glembocki OJ, Livenere JE, Tumkur TU, Kitur JK, Zhu G, Wells B, Podolskiy VA, Noginov MA (2013) Hyperbolic and plasmonic properties of silicon/Ag aligned nanowire arrays. Opt Express 21:14962–14974
13. Schmidt OG, Eberl K (2001) Nanotechnology: thin solid films roll up into nanotubes. Nature 410:168
14. Cavallo F, Songmuang R, Schmidt OG (2008) Fabrication and electrical characterization of Si-based rolled-up microtubes. Appl Phys Lett 93:143113
15. Müller C, Khatri MS, Deneke C, Fähler S, Mei YF, Urena EB, Schmidt OG (2009) Tuning magnetic properties by roll-up of Au/Co/Au films into microtubes. Appl Phys Lett 94:102510
16. Deneke C, Schmidt OG (2004) Real-time formation, accurate positioning, and fluid filling of single rolled-up nanotubes. Appl Phys Lett 85:2914–2916

17. Thurmer DJ, Deneke C, Mei YF, Schmidt OG (2006) Process integration of microtubes for fluidic applications. Appl Phys Lett 89: 223507
18. Deneke C, Schmidt OG (2006) Structural characterization and potential x-ray waveguiding of a small rolled-up nanotube with a large number of windings. Appl Phys Lett 89:123121
19. Schwaiger S, Bröll M, Krohn A, Stemmann A, Heyn C, Stark Y, Stickler D, Heitmann D, Mendach S (2009) Rolled-up three-dimensional metamaterials with a tunable plasma frequency in the visible regime. Phys Rev Lett 102:163903
20. Yin Y, Qiu T, Ma L, Lang XZ, Zhang Y, Huang GS, Mei YF, Schmidt OG (2012) Exploring rolled-up Au–Ag bimetallic microtubes for surface enhanced Raman scattering sensor. J Phys Chem C 116(48):25504–25508
21. Songmuang R, Deneke C, Schmidt OG (2006) Rolled-up micro- and nanotubes from single-material thin films. Appl Phys Lett 89:223109
22. Mei YF, Huang GS, Solovev AA, Ureña EB, Mönch I, Ding F, Reindl T, Fu RKY, Chu PK, Schmidt OG (2008) Versatile approach for integrative and functionalized tubes by strain engineering of nanomembranes on polymers. Adv Mater 20:4085–4090
23. Huang GS, Kiravittaya S, Bolaños Quiñones VA, Ding F, Benyoucef M, Rastelli A, Mei YF, Schmidt OG (2009) Optical properties of rolled-up tubular microcavities from shaped nanomembranes. Appl Phys Lett 94:141901
24. Huang GS, Mei YF (2012) Thinning and shaping solid films into functional and integrative nanomembranes. Adv Mater 24:2517–2546
25. Wan GJ, Solovev AA, Huang GS, Maitz MF, Huang N, Mei YF (2012) Dynamic curvature control of rolled-up metal nanomembranes activated by magnesium. J Mater Chem 22: 12983–12987
26. Qiu T, Zhang WJ, Lang XZ, Zhou YJ, Cui TJ, Chu PK (2009) Controlled assembly of highly Raman-enhancing silver nanocap arrays templated by porous anodic alumina membranes. Small 5:2333–2337
27. Kneipp K, Kneipp H, Kneipp J (2006) Surface-enhanced Raman scattering in local optical fields of silver and gold nanoaggregatess from single-molecule Raman spectroscopy to ultrasensitive probing in live cells. Acc Chem Res 39(7):443–450
28. Wang YQ, Yan B, Chen LX (2013) SERS tags: novel optical nanoprobes for bioanalysis. Chem Rev 113(3):1391–1428
29. Lawandy NW (2004) Localized surface plasmon singularities in amplifying media. Appl Phys Lett 85:5040–5042
30. Noginov MA, Zhu G, Bahoura M, Adegoke J, Small CE (2006) Enhancement of surface plasmons in an Ag aggregate by optical gain in a dielectric medium. Opt Lett 31:3022–3024
31. See supplemental material for SERS enhancement factor calculation
32. Kennedy BJ, Spaeth S, Dickey M, Carron KT (1999) Determination of the distance dependence and experimental effects for modified SERS substrates based on self-assembled monolayers formed using alkanethiols. J Phys Chem B 103(18):3640–3646